

New Method for Estimating the Extent of Curing of Thermosetting Prepregs

S. M. Sabzevari, S. Alavi-Soltani, B. Minaie

Department of Mechanical Engineering, Wichita State University, Wichita, Kansas 67260

Received 28 July 2010; accepted 12 October 2010

DOI 10.1002/app.33616

Published online 25 February 2011 in Wiley Online Library (wileyonlinelibrary.com).

ABSTRACT: Here, we propose a new method for estimating the extent of curing of thermosetting prepregs. In the proposed method, the extent of curing is estimated with the *curing index* (C_i), defined as the ratio of the glass-transition temperature (T_g) to the ultimate glass-transition temperature of the material. The advantages of this new method over the conventional degree of conversion (α) for estimating the extent of curing of thermosetting prepregs are discussed in detail. C_i and α of a toughened epoxy prepreg (977-2 unidirectional) were obtained for a wide range of isothermal curing temperatures with a differential scanning calorimeter. The ultimate heat of reaction varied

inconsistently with decreasing curing temperature; this resulted in erratic behavior of α . However, C_i provided a more consistent estimate of the extent of curing because T_g , unlike α , did not need to be modified on the basis of the curing history of the material and was measured directly with the heat-flow data from differential scanning calorimetry. © 2011 Wiley Periodicals, Inc. *J Appl Polym Sci* 121: 883–891, 2011

Key words: composites; curing of polymers; differential scanning calorimetry (DSC); glass-transition temperature; thermosets

INTRODUCTION

The curing of thermosetting resins and composite materials has been studied by many investigators over the years. In most of these studies, the extent of curing, as a result of crosslinking reactions and polymerization, is estimated by a thermal property, namely, the degree of conversion (α). For an uncured resin, α is equal to zero, whereas for a fully cured resin, α is equal to 1.

Although α estimates the extent of curing of many thermosetting resins with sufficient accuracy and consistency, it is not as accurate or consistent for estimating the extent of curing of thermosetting composite materials such as prepregs. This is mainly because the curing mechanism of thermosetting composite materials is more complicated than that of thermosetting resins. For example, the moisture absorption, fiber sizing, and initial degree of conversion (α_0) affect the curing behavior and postcuring properties of prepregs.^{1–3} Moreover, the flowability of resin in the prepreg significantly affects the rate of crosslinking reactions during curing. In other

words, the presence of fibers in a thermosetting prepreg reduces the availability of participating reactants in curing reactions and, consequently, results in a lower rate of reaction and a lower value of ultimate heat of reaction (H_U). As such, it is necessary to find a more sophisticated method to estimate the extent of curing of thermosetting composite materials. This new method should address the issues associated with the complicated mechanism of curing in composite materials and eliminate the uncertainties associated with the calculations.

The curing kinetics of thermosetting resins is often modeled with $d\alpha/dt$ versus α data.^{4–18} The modeling of curing kinetics makes it possible to predict the behavior of the material during curing. The crosslinking reactions of thermosetting resins are exothermic. It is possible to measure the heat released from exothermic curing reactions with differential scanning calorimetry (DSC). The measured heat is subsequently used to calculate α . One can calculate α at time t by dividing the amount of heat released up to time t ($H(t)$) by H_U , obtained by the integration of the exothermic heat-flow curve over the entire curing time. As we explain later, the complementary residual heat of reaction (H_R) can also be used to calculate α .

Calculating the heat of reaction is not an easy task. This is mainly because of the uncertainties associated with finding the heat-flow integration baseline and the integration starting and ending points. Several methods have been developed for calculating α , each of which uses a different equation.

Correspondence to: B. Minaie (bob.minaie@wichita.edu).

Contract grant sponsor: National Aeronautics and Aerospace Administration; contract grant number: NNX09AO58A.

Contract grant sponsor: Kansas Technology and Enterprise Corp.

In the first method, one calculates α by dividing $H(t)$ by a constant H_{U} , which is assumed to be a material property:^{1,3-5,8,19,20}

$$\alpha(t) = \frac{1}{H_{U,dyn}} \int_0^t \left(\frac{dH(t)}{dt} \right) dt \quad (1)$$

where $dH(t)/dt$ is the rate of heat generation (heat flow) and $H_{U,dyn}$ is the ultimate heat of reaction obtained from dynamic scanning. Equation (1) has commonly been used to obtain α as a continuous function of the curing time.

As we show later, H_U of thermosetting prepregs is not necessarily constant and may vary, depending on the temperature profile used to cure the material. As such, this method does not address the uncertainties associated with the calculation of H_U for prepregs.

In the second method, α is obtained with the following equation:^{5,21,22}

$$\alpha = 1 - \frac{H_R}{H_{U,dyn}} \quad (2)$$

where H_R is the residual heat of reaction obtained by dynamic scanning performed immediately after the end of the curing cycle.

Equation (2) provides only a single value for α , that is, the final α for a cured sample. As such, to obtain α throughout the entire curing cycle, the curing time should be divided into several shorter time periods. For each time period, at least one sample should be cured to determine the corresponding residual heat. In contrast, the data obtained from running only one DSC sample with an arbitrary curing cycle is sufficient to obtain α with eq. (1) as a continuous function of time during curing, provided that the heat-flow baselines and $H_{U,dyn}$ are known. It is, however, better to assess α obtained from eq. (1) with α obtained from eq. (2), especially for complicated curing profiles, such as multistage curing cycles.

In the third method, the isothermal curing α which is called β , which is a modified curing parameter introduced by Hubert¹⁰ and Kim et al.¹ is used to facilitate the modeling of curing behavior using the already established curing kinetics models:

$$\beta(t) = \frac{1}{H_T} \int_0^t \left(\frac{dH(t)}{dt} \right) dt \quad (3)$$

where H_T is the total heat of reaction obtained from the isothermal scanning of thermosetting resins with an infinite curing time.

This method does not account for H_R . As such, the final value of β for curing at any isothermal temperature is equal to 1. However, H_T of thermosetting resins cured at isothermal curing temperatures (T_{iso} 's) of less than the ultimate glass-transition temperature of the material ($T_{g\infty}$) is smaller than $H_{U,dyn}$ even if the curing time tends to infinity.

The shortcoming of the third method is addressed by the inclusion of H_U in the calculations. The modified degree of conversion $\alpha(t)$ was obtained by the substitution of eq. (1) into eq. (3):

$$\alpha(t) = \beta(t) \frac{H_T}{H_U} \quad (4)$$

where H_T/H_U is the relative maximum α to be used in the curing kinetics models.

All of the abovementioned methods were originally introduced to determine α for thermosetting resins, where α_0 was assumed to be zero. In thermosetting prepregs, however, the resin is partially cured for the ease of handling and processing. As a result, α_0 is not zero. As such, α of prepregs should be modified with eq. (5) to account for α_0 .^{3,16}

$$\alpha_m = \alpha_0 + (1 - \alpha_0)\alpha \quad (5)$$

where α is the degree of conversion obtained from DSC on the basis of eq. (1) or (2), α_0 is the initial degree of conversion of a prepreg, and α_m is the modified degree of conversion changes significantly in the early stages of curing where α is far below unity. Furthermore, α_m is more sensitive to higher values of α_0 when the prepreg is isothermally cured at temperatures lower than $T_{g\infty}$.

One-to-one relationship between T_g and α

A unique one-to-one relationship has been established between T_g and α for many thermosetting materials. This relationship is often stated by the DiBenedetto relation.^{5,12,23} Equation (6) shows the DiBenedetto relation in the form of Pascault and Williams:²⁴

$$T_g = \frac{(1 - \alpha)T_{g0} + \lambda\alpha T_{g\infty}}{(1 - \alpha) + \lambda\alpha} \quad (6)$$

where T_{g0} and $T_{g\infty}$ are the glass-transition temperatures of the resin at the initial and final stages of curing, respectively, and λ is an adjustable, structure-dependent factor ranging from 0 to 1.

In this study, the curing kinetics of a thermosetting prepreg were studied at various T_{iso} 's with DSC. The extent of curing of the prepreg was investigated with the abovementioned definitions of α , and a new parameter obtained from the T_g data was

introduced to estimate the extent of curing of the thermosetting prepregs.

EXPERIMENTAL

A commercial carbon fiber prepreg [Cycom 977-2 unidirectional (UD), Cytec Engineered Materials Inc., Tempe, AZ] was used in this study. This toughened epoxy resin prepreg was formulated for autoclave or press molding. The manufacturer-recommended curing cycle for 977-2 UD is isothermal curing at 177°C for 180 min. The prepregs manufactured by the 977-2 resin system had a long outlife, appropriate for the fabrication of large structures,²⁵ and have been used extensively in the construction of modern aircraft, such as the Airbus A380 and Boeing 787.²⁶ The carbon fiber used in 977-2 UD was HexTow IM7. It is a continuous, high-performance, intermediate modulus (276 GPa), PAN-based (polyacrylonitrile) carbon fiber manufactured by Hexcel.²⁷

We conducted thermal experiments with a TA Instruments Q2000 differential scanning calorimeter. Before testing the prepreg samples, we calibrated the DSC instrument with a high-purity indium standard reference sample. Dry nitrogen (99.99% purity) was used as the purge gas with a constant flow rate of 50 mL/min. The prepreg samples, consisting of four layers of prepreg with a diameter of 4.9 mm and a total weight of about 12 mg, were encapsulated in standard Tzero aluminum pans provided by TA Instruments. The investigation of the effect of the prepreg layup and stacking sequence was beyond the scope of this study. A similar empty pan was used as the reference. The samples were selected from the same batch of prepregs and cured in the DSC cell. All of the experiments were conducted within a short period of time (ca. 2 weeks) to eliminate the effect of aging on the prepreg samples. For T_g measurement, the prepreg samples were partially cured in the DSC cell at different T_{iso} 's, which ranged from 140 to 200°C with an increment of 10°C. The curing times for each T_{iso} were between 5 and 1000 min. Similar experiments were carried out to measure α .

All of the isothermal curing cycles were followed by two dynamic scans from -20 to 290°C. The first dynamic scan was performed to determine T_g and H_R . The second dynamic scan was performed to ensure all of the exothermic reactions had occurred and that no additional unreacted functional groups remained in the samples.

Two different heating rates were used for dynamic scans depending on the property measured. For T_g measurement, the dynamic scans were performed at 10°C/min according to ASTM E 1356-03 (Standard Test Method for Assignment of the Glass-Transition Temperature by DSC). However, because lower heating rates give more time to the material to

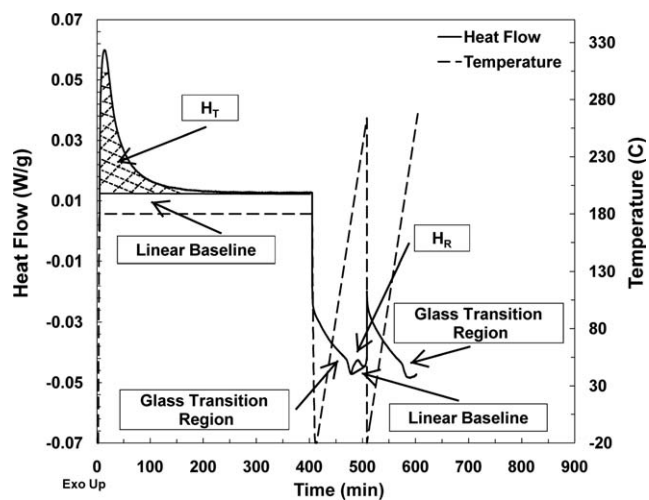


Figure 1 Heat-flow versus curing time plot demonstrating various curing events during a DSC experiment at $T_{iso} = 180^\circ\text{C}$.

release the residual heat of curing, the dynamic scans for H_R measurement were carried out at 3°C/min. This rate was obtained after several trials at different heating rates. The value of T_g changed slightly when the heating rate was varied. In general, the glass-transition region appeared as an endothermic shift in the plot of the heat-flow or heat capacity (C_p) versus curing time or curing temperature. In this study, T_g was defined as the temperature corresponding to the half-height point of the step transition in the heat-flow versus time curve. TA Instruments Universal Analysis 2000 software was used to obtain T_g with the heat-flow data from DSC.

Figure 1 illustrates the rate of heat generation versus curing time during an isothermal DSC scan at 180°C. The heat-flow data was mass-normalized to eliminate the effect of the sample size on the results. The exothermic peaks of the heat-flow during isothermal scanning and postcuring dynamic scanning are shown in the figure, as is the glass-transition region. These peaks were indicative of the heat released by crosslinking reactions during curing.

Two T_g 's are shown in Figure 1. The first T_g , which occurred during the first dynamic scan, signified the T_g of the isothermally cured sample, whereas the second T_g , which occurred during the second dynamic scan, signified the maximum obtainable glass-transition temperature for the cured sample ($T_{g\infty}$). Figure 2 shows how T_g was determined. Although no additional chemical reactions occurred after the glass-transition in the second dynamic scan, we observed that the second T_g was not necessarily equal to $T_{g\infty}$. For example, the first and second T_g values of the five samples cured at 190°C are shown in Table I. As shown in the table, the second T_g of all of the samples, except for that of sample 5, was less than $T_{g\infty}$.

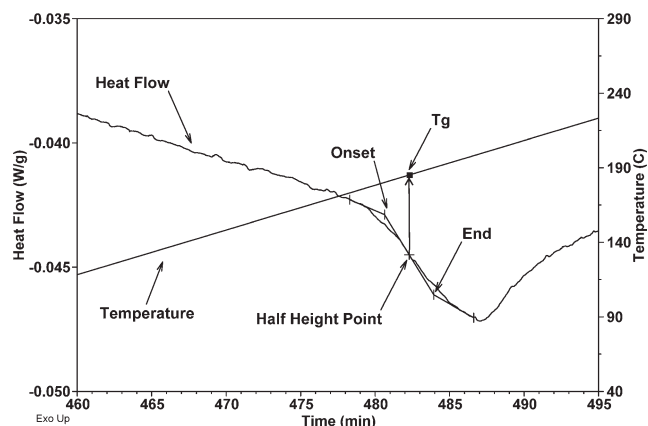


Figure 2 Determination of T_g with the heat-flow data from DSC.

For an isothermal curing cycle, H_U is defined as the sum of H_T and the corresponding H_R which is called $H_{U,iso}$.^{2,8}

$$H_{U,iso} = H_T + H_R \quad (7)$$

As shown in Figure 1, H_T was calculated by integration of the exothermic heat-flow peak. The heat-flow plateau was used as the baseline for integration. To find the integration starting point, the plateau line was extrapolated until it crossed the heat-flow curve before the peak. H_R was obtained with a linear baseline. Figure 3 illustrates the heat-flow during a dynamic scan. We calculated $H_{U,dyn}$ by finding the area enclosed by the heat-flow curve and a linear baseline. The baseline was constructed by a line that connected two points: (1) the point at which the heat-flow curve started to rise toward the peak and (2) the point at which the minimum heat-flow after the peak occurred.

RESULTS AND DISCUSSION

Heat of reaction

We observed that the values of H_U of 977-2 UD obtained from different curing cycles differed signifi-

TABLE I
Thermal Properties of Five Prepreg Samples Cured at $T_{iso} = 190^\circ\text{C}$ for 300 min

Sample	T_{g0} (°C)	T_g (°C)	T_{gf} (°C)	H_T (J/g)	H_R (J/g)	$H_{U,iso}$ (J/g)
1	-4	191	192	144.2	1.1	145.3
2	-5	189	189	158.6	0.7	159.3
3	-5	197	199	139.4	1.8	141.2
4	-4	193	196	156.8	1.7	158.5
5	-6	197	200	140.2	1.8	142.0

T_{gf} : final T_g of the sample, which is not necessarily equal to $T_{g\infty}$ (200°C).

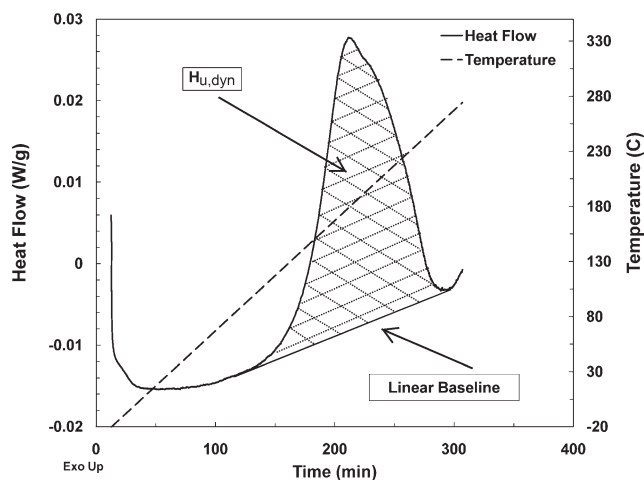


Figure 3 Calculation of $H_{U,dyn}$ through the integration of the heat-flow curve using a linear baseline.

cantly. As such, several isothermal and dynamic scans were carried out on the samples of 977-2 UD to further investigate the variation of H_U under different testing conditions.

Heat of reaction from dynamic scanning

The average value of $H_{U,dyn}$ obtained from the dynamic scanning of five 977-2 UD samples at a rate of $1^\circ\text{C}/\text{min}$ was 146.4 ± 1.0 J/g. The obtained $H_{U,dyn}$ was for the prepreg system consisting of fiber and resin. To calculate H_U of the resin, the resin mass content of the prepreg was measured by acid digestion according to ASTM D 3171 (Standard Test Methods for Constituent Content of Composite Materials). The mass content of the resin was found to be 33.2%. Therefore, after we compensated for the obtained heat of reaction for the fiber mass content of the prepreg, $H_{U,dyn}$ of the resin was calculated to be about 441 J/g.

Heat of reaction from isothermal scanning

Figures 4–6 show the variations of H_T , H_R , and $H_{U,iso}$ with respect to T_{iso} . As shown in these figures, samples cured at T_{iso} 's far below $T_{g\infty}$ of the material (200°C) had smaller H_T values and, consequently, greater H_R values. We could explain such behavior considering the fact that the lower curing temperatures do not activate the entire reactive molecules of thermosetting resins. Moreover, the greater H_R at lower T_{iso} 's indicated incomplete curing reactions, even with infinite curing time.

Figure 6 illustrates the discrepancy between the values of H_U obtained from the dynamic scans and those obtained from the isothermal scans. Because the x axis of the figure is T_{iso} , the upper and lower limits of the standard deviation of $H_{U,dyn}$ are represented with two lines. As shown in this

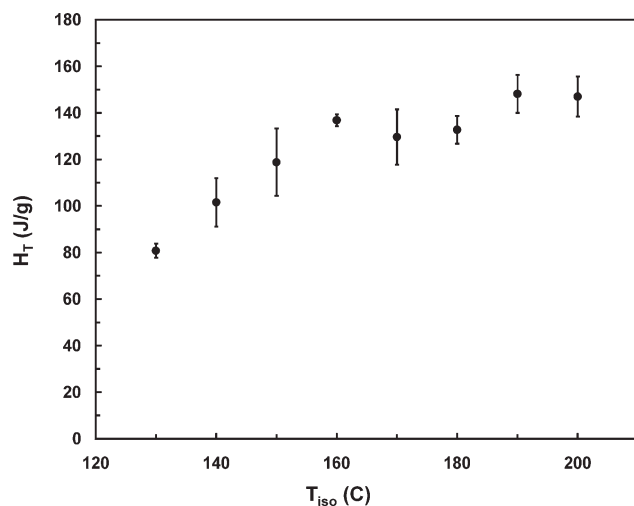


Figure 4 Variation of H_T with T_{iso} . The mean values are presented with error bars representing the standard deviation.

figure, $H_{U,iso}$ inconsistently varied with decreasing T_{iso} . Furthermore, $H_{U,iso}$ varied even for the samples of the same prepreg cured with an identical curing cycle. Because the heat-flow data measured by DSC was mass-normalized, such a discrepancy may have been due to a slight variation in the resin/fiber content from one sample to another. The overall decrease of $H_{U,iso}$ with T_{iso} was a result of early vitrification, which prevented the advancement of chemical reactions by separating the nonactivated reaction sites from the fully or partially vitrified zones. This limited the reinitiation of the curing reactions during postcuring dynamic scanning, which in turn, led to the erratic behavior of α .

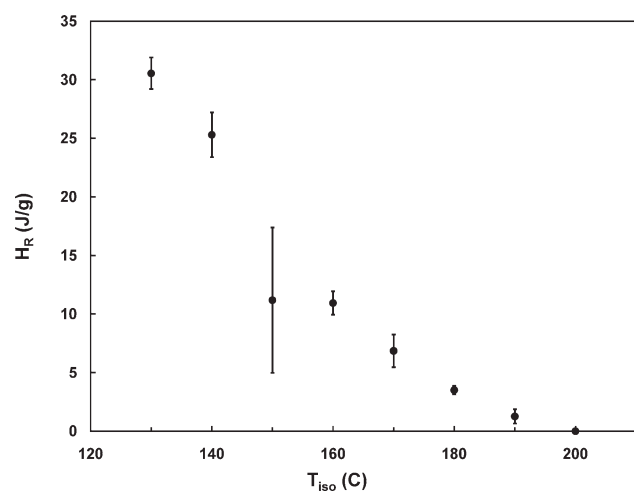


Figure 5 Variation of H_R with T_{iso} . The data was obtained by the postcuring of the isothermally cured samples shown in Figure 3. The mean values are presented with error bars representing the standard deviation.

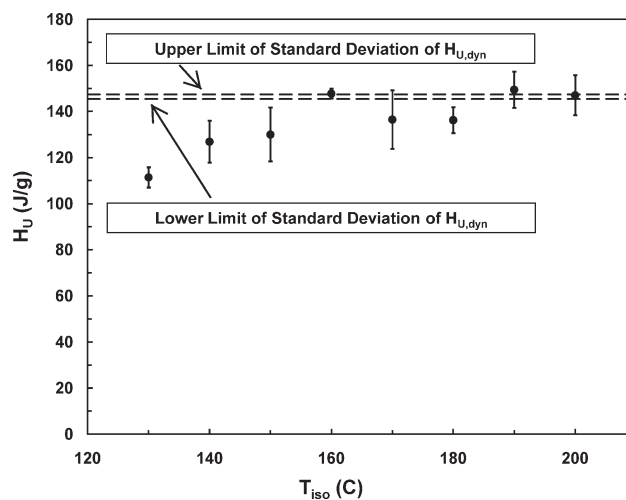


Figure 6 Variation of $H_{U,iso}$ with T_{iso} . The mean values are presented with error bars representing the standard deviation. The dashed lines represent the upper and lower limits of the standard deviation of $H_{U,dyn}$.

Inconsistency in the heat of reaction

Figure 7 illustrates the heat-flow during isothermal curing at 190°C for five 977-2 UD samples. The discrepancy in H_T (and, subsequently, in $H_{U,iso}$) was due to the difference in the shape of the heat-flow curves, both at the peak and before the plateau was reached. This difference could have been due to the variation in the concentration of the monomers and the difference in the resin-to-fiber ratio in the samples. Table I shows the variations in the T_g and heat of reaction for all five samples. For example, the T_g and H_T values of samples 2 and 5 were 189 and 197°C and 158.6 and 140.2 J/g, respectively; this reveals that a higher heat of reaction did not necessarily result in a higher T_g .

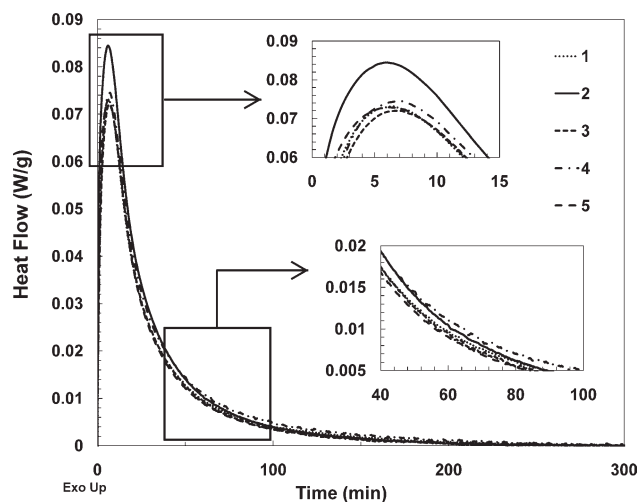


Figure 7 Progress of the chemical reactions for five prepreg samples cured at $T_{iso} = 190^\circ\text{C}$ in a plot of the heat flow versus curing time.

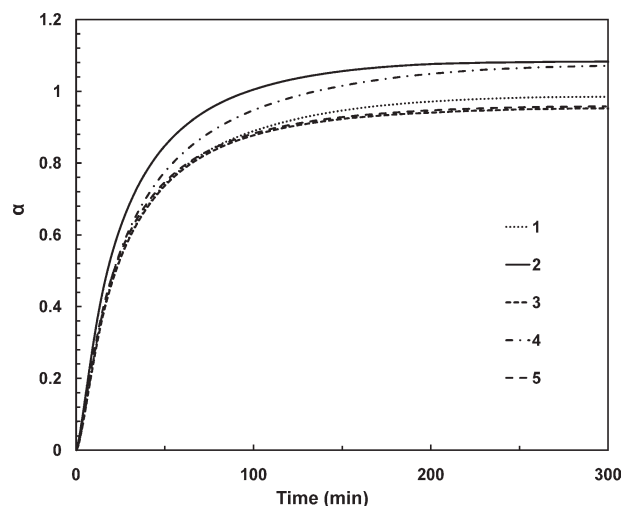


Figure 8 Variation of α versus curing time for five prepreg samples cured at $T_{\text{iso}} = 190^{\circ}\text{C}$. The data was calculated with eq. (1) on the basis of $H_{U,\text{dyn}}$.

Degree of conversion α

In the previous sections, we showed that the heat of reaction inconsistently changed with the change in curing temperature. This, in turn, resulted in an erratic behavior of α . In the following section, we discuss different possible scenarios to study the change in α with the variation of the heat of reaction.

Case 1: Using eq. (1)

With eq. (1), one calculates $\alpha(t)$ by dividing $H(t)$ by $H_{U,\text{dyn}}$ (146.4 J/g), which is separately obtained from a dynamic scan. Figure 8 demonstrates α versus the curing time for five prepreg samples, the heat-flow curves of which are shown in Figure 7. Because the same $H_{U,\text{dyn}}$ was used to normalize the heat-flow integration for all samples, α of the two samples became more than 1 at the final stages of curing. Obviously, the obtained α for these two samples was not acceptable. In addition, the final α for the five samples showed up to 20% variation. This demonstrated that the inconsistency in H_T directly affected the obtained α .

The calculation of heat of reaction with eq. (1) is not a simple task, particularly for multistage curing cycles. This is mainly due to uncertainties associated with the construction of the heat-flow integration baseline. One can obtain the baseline either by using the heat-flow plateau or by obtaining the heat-flow of the same sample undergoing a secondary curing cycle identical to the original curing profile. The former constrains application of eq. (1) to one-stage curing cycles. The latter is applicable to every type of curing cycle; however, the baseline constructed by this method suffers from other issues. First, the material must be completely cured with no residual

heat before it undergoes the secondary curing cycle. Partially cured samples release heat during the secondary curing cycle; therefore, their heat-flow curve cannot be used to construct the baseline. Second, even if the sample is fully cured, the baseline obtained from the secondary curing cycle is not similar to that of the original curing cycle because of the change in C_p of the sample. C_p of thermosetting resins may vary with α . The change in C_p alters the heat-flow curve (and, as a result, the baseline) for fully cured samples compared to that of uncured samples. The abovementioned limitations and issues have led many researchers to use eq. (2) instead of eq. (1).

Case 2: Using eq. (1) with H_U obtained from each experiment

Some researchers calculate α using H_U from the same experiment, that is, the sum of the heat from isothermal scanning and the corresponding residual heat from dynamic scanning ($H_{U,\text{iso}}$). For this method, Figure 9 shows the graph of α versus the curing time for the same samples shown in Figure 7. As shown on the graphs, this method produces more consistent results than those shown in Figure 8, where α was calculated with $H_{U,\text{dyn}}$. However, this approach does not precisely represent the state of curing of a material because of the discrepancy observed in H_U , shown in Figure 6. In most cases, this method results in an overestimation of α because $H_{U,\text{iso}}$ is less than $H_{U,\text{dyn}}$. In this study, the difference between these values was called the *lost heat of reaction* (H_L), or error. H_L was more obvious at curing temperatures far below $T_{g\infty}$. As mentioned previously, this was because of the early vitrification of the polymer chains at low curing temperatures; this, consequently,

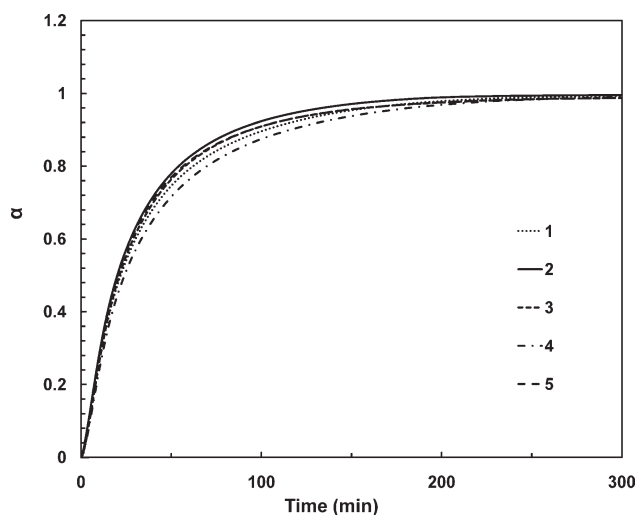


Figure 9 Variation of α versus curing time for five prepreg samples cured at $T_{\text{iso}} = 190^{\circ}\text{C}$. The data was calculated with eq. (1) on the basis of $H_{U,\text{iso}}$ from each experiment.

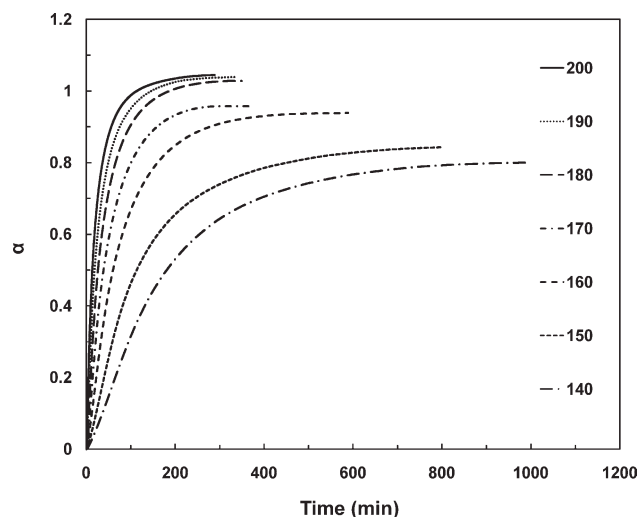


Figure 10 Progress of α with curing time at T_{iso} values ranging from 140 to 200°C. The calculations were performed with eq. (1) on the basis of $H_{U,\text{dyn}}$. Some plateaus exceeded unity because of the shortcoming of the calculation method.

prevents reinitiation of the chemical reactions during dynamic scanning. Accordingly, $H_{U,\text{dyn}}$ could be written as the sum of H_T , H_R , and H_L :

$$H_{U,\text{dyn}} = H_{U,\text{iso}} + H_L = H_T + H_R + H_L \quad (8)$$

$$\alpha(t) = \frac{H(t)}{H_{U,\text{iso}}} = \frac{H(t)}{H_{U,\text{dyn}} - H_L} \quad (9)$$

It is clear that eq. (9) overestimates α by ignoring H_L .

Case 3: Using eq. (2)

This method is useful for calculating the final α , regardless of the type of curing cycle, by invoking the value of H_R from the original experiment and H_U from a separate dynamic scan. As mentioned before, eq. (2) provides only α at the end of curing cycle. As such, several experiments need to be performed to obtain α during curing by eq. (2). Moreover, eq. (2) results in an overestimation of α by adding H_L to the isothermal heat of reaction, as shown in eq. (10):

$$\alpha = 1 - \frac{H_R}{H_{U,\text{dyn}}} = \frac{H_T + H_L}{H_{U,\text{dyn}}} \quad (10)$$

Case 4: Using eqs. (3) and (4)

α obtained from eq. (3) is not a proper measure of the extent of curing because the β curve approaches 1 for any arbitrary T_{iso} ; this indicates the achievement of a fully cured state. However, the fully cured state is never achieved by thermosetting res-

ins cured at T_{iso} 's well below $T_{g\infty}$. As mentioned earlier, eq. (3) was only introduced to simplify the use of the reaction rate equations for modeling purposes.

Although eq. (4) modifies the results obtained from eq. (3); α obtained with this equation still suffers from the same issues as explained for eq. (1), that is, the erratic behavior of α .

Finally, α calculated with eqs. (1)–(4) needs to be modified to account for α_0 of the prepreg. Because α_0 is usually unknown for prepregs, it is assumed to be zero. As such, the real α is underestimated.

T_g - α relationship

The variations of α and T_g of 977-2 UD as functions of the curing time and curing temperature are shown in Figures 10 and 11. Figure 10 was obtained with eq. (1) and $H_{U,\text{dyn}}$ (146.4 J/g) to illustrate the overall behavior of α , regardless of the accuracy of data. The step transition observed in Figure 11 with the progress of $T_g(t)$ at curing temperatures above 180°C revealed the existence of a secondary curing agent or a modifier.¹²

Figure 12 shows the relationship between T_g and α . As shown, there was a unique one-to-one relationship between these parameters. Moreover, the DiBenedetto model, obtained with eq. (6), closely followed the experimental data. The value of λ was calculated to be 0.60 for 977-2 UD.

Curing index (C_i): A better estimate of the extent of curing for thermosetting prepregs

As shown previously, the current methods for calculating α resulted in either overestimation or underestimation of the extent of curing, regardless of the

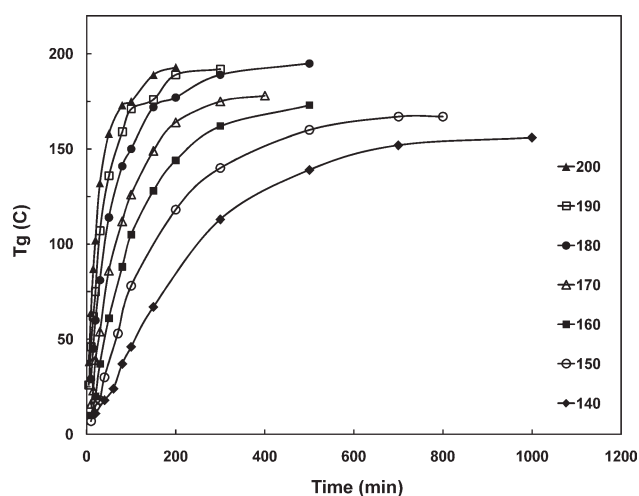


Figure 11 Progress of $T_g(t)$ with curing time at T_{iso} values ranging from 140 to 200°C. The symbols represent the data points.

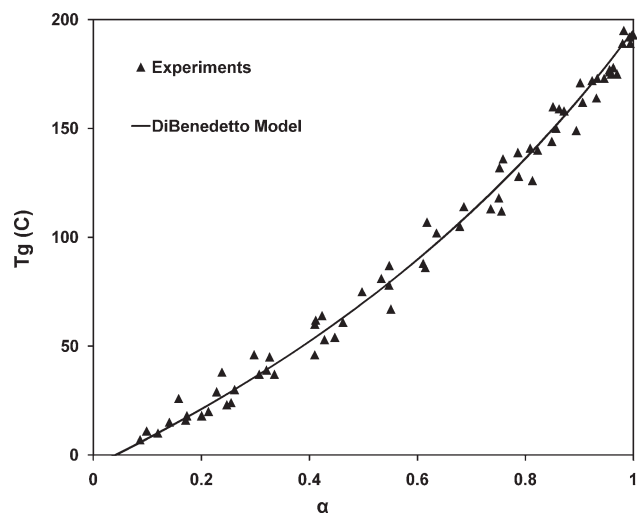


Figure 12 T_g versus α from the experiment and the modeling data obtained with the DiBenedetto relationship.

accuracy of the heat-flow data from DSC. As such, none of these methods accurately estimated the extent of curing of the thermosetting prepregs. Nevertheless, Figures 10 and 11 reveal that $\alpha(t)$ and $T_g(t)$ had similar behavior at various curing temperatures. Moreover, the existence of a strong relationship between T_g and α , shown in Figure 12, demonstrated that T_g had the capability of estimating the extent of curing for the thermosetting prepregs. As such, to address the shortcomings of the conventional α , we propose a new method for estimating the extent of curing of thermosetting prepregs. In the proposed method, the extent of curing is esti-

mated with C_i , which is the normalized T_g and is defined as follows:

$$C_i = \frac{T_g}{T_{g\infty}} \quad (11)$$

where T_g is the glass-transition temperature and $T_{g\infty}$ is the ultimate glass-transition temperature of the prepreg. Both T_g and $T_{g\infty}$ should be obtained with the same heating rate. $T_{g\infty}$, the maximum achievable glass-transition temperature of the material, is a constant material property. To obtain $T_{g\infty}$ for 977-2 UD, the prepreg samples were initially cured at a reasonably low heating rate (e.g., 1°C/min) to ensure completeness of the curing reactions; then, $T_{g\infty}$ was measured with dynamic scanning performed at 10°C/min.

To obtain C_i for the entire curing cycle, the curing time should be divided into several shorter time periods. For each time period, one sample should be cured to determine the corresponding T_g . For example, Table II contains the time periods and corresponding $T_g(t)$ values for the same samples shown in Figure 11. To obtain more data points, the time periods should be shorter. The required number of time periods and the duration of each should be determined on the basis of several considerations, including the material type and the complexity of the curing cycle.

As shown in Table I, H_T , H_R , $H_{U,iso}$ (subsequently, α), and T_g varied for the samples of the same prepreg cured with the same curing cycle. This means that an accurate estimation of the extent of curing by any of the aforementioned methods was not

TABLE II
 $T_g(t)$ (°C) for Different T_{iso} 's

Curing time (min)	T_{iso} (°C)						
	140	150	160	170	180	190	200
5	N/A	N/A	N/A	N/A	N/A	26	38
10	N/A	7	10	16	29	46	64
15	N/A	N/A	N/A	23	45	62	87
20	11	15	20	39	60	75	102
30	N/A	18	37	54	81	107	132
40	18	30	N/A	N/A	N/A	N/A	N/A
50	N/A	N/A	61	86	114	136	158
60	24	N/A	N/A	N/A	N/A	N/A	N/A
70	N/A	53	N/A	N/A	N/A	N/A	N/A
80	37	N/A	88	112	141	159	173
100	46	78	105	126	150	171	175
150	67	N/A	128	149	172	176	189
200	N/A	118	144	164	177	189	193
300	113	140	162	175	189	192	N/A
400	N/A	N/A	N/A	178	N/A	N/A	N/A
500	139	160	173	N/A	195	N/A	N/A
700	152	167	N/A	N/A	N/A	N/A	N/A
800	N/A	167	N/A	N/A	N/A	N/A	N/A
1000	156	N/A	N/A	N/A	N/A	N/A	N/A

N/A, not available.

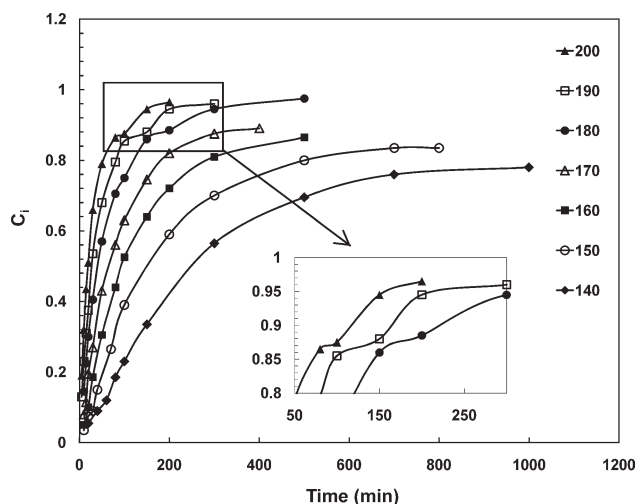


Figure 13 Progress of C_i with curing time at T_{iso} values ranging from 140 to 200°C.

possible. However, the use of C_i for estimating the extent of curing eliminated many uncertainties associated with the calculation of α . Some of the advantages of T_g over α are as follows:

- Obtaining the heat of reaction needed for calculating α is not an easy task, particularly for complex curing cycles, because of the difficulty of constructing the heat-flow baseline. In contrast, T_g can be measured directly with heat-flow data from DSC at any arbitrary point during curing.
- A small change in the heat-flow integration starting and ending points considerably affects the obtained value of the heat of reaction needed to calculate α . However, the choice of starting and ending points of the glass-transition region barely affects the obtained value of T_g .
- Although α of prepregs should be modified to account for α_0 , T_g does not need to be modified on the basis of the curing history of the material.
- Although α can only be measured by DSC, T_g and, therefore, C_i can be measured by DSC and other instruments, such as dynamic mechanical analysis.

Figure 13 illustrates the progress of C_i with the curing time at different T_{iso} 's. As mentioned previously, the step transition observed in the C_i curve at curing temperatures above 180°C revealed the existence of a secondary curing agent or modifier. This shows that C_i can provide information about the constituents of the resin system in addition to estimating the extent of curing.

CONCLUSIONS

In this study, we showed that none of the existing methods for calculating α consistently and accurately estimated the extent of curing of thermosetting pre-

pregs. This was due to the inconsistency in the calculated heat of reaction obtained at different T_{iso} 's and to the difficulty of constructing the heat-flow baseline. As a result, for thermosetting prepregs, α may not be a proper measure of the extent of curing. In contrast, C_i , defined as the ratio of T_g to $T_{g\infty}$, provided a more consistent estimate of the extent of curing of the thermosetting prepregs because both T_g and $T_{g\infty}$ were measured directly with the heat-flow data from DSC and did not need to be modified on the basis of the curing history of the material. C_i can be used to estimate the extent of curing of autoclave and out-of-autoclave prepregs and neat resins. However, C_i , unlike α , cannot be measured in real time.

References

1. Kim, J.; Moon, M. J.; Howell, J. R. *J Compos Mater* 2002, 36, 2479.
2. Sun, L. Ph.D. Thesis, Louisiana State University, 2002.
3. Hargis, M.; Grady, B. P.; Aktas, L.; Bomireddy, K. R.; Howsman, S.; Altan, M. C.; Rose, T.; Rose, H. *J Compos Mater* 2006, 40, 873.
4. Wisanrakkit, G.; Gillham, J. K. *J Appl Polym Sci* 1990, 41, 1895.
5. Wisanrakkit, G.; Gillham, J. K. *J Appl Polym Sci* 1990, 41, 2885.
6. Mantell, S. C.; Ciriscioli, P. R.; Almen, G. *J Reinf Plast Compos* 1995, 14, 847.
7. Vilas, J. L.; Laza, J. M.; Garay, M. T.; Rodriguez, M.; Leon, L. M. *J Appl Polym Sci* 2001, 79, 447.
8. Lee, W.; Loos, A. C.; Springer, G. S. *J Compos Mater* 1982, 16, 510.
9. Gao, J.; Li, L.; Deng, Y.; Gao, Z.; Xu, C.; Zhang, M. *J Therm Anal Calorim* 1997, 49, 303.
10. Hubert, P.; Johnson, A.; Poursartip, A.; Nelson, K. *Int SAMPE Symp* 2001, 46, 2341.
11. Flores, J. D. M.Sc. Thesis, Wichita State University, 2006.
12. Simon, L.; Gillham, J. K. *J Appl Polym Sci* 1994, 53, 709.
13. Ramis, X.; Cadenato, A.; Morancho, J. M.; Salla, J. M. *Polymer* 2003, 44, 2067.
14. Mijovic, J.; Kenny, J. M.; Nicolais, L. *Polymer* 1993, 34, 207.
15. Enns, J. B.; Gillham, J. K. *J Appl Polym Sci* 1983, 28, 2567.
16. Dykeman D, Ph.D. Thesis, University of British Columbia, 2008.
17. Cole, K. C. *Macromolecules* 1991, 24, 3093.
18. Seifi, R.; Hojjati, M. *J Compos Mater* 2005, 39, 1027.
19. Costa, M. L.; Botelho, E. C.; Rezende, M. C. *J Mater Sci* 2006, 41, 4349.
20. Loos, A. C.; Springer, G. S. *J Compos Mater* 1983, 17, 135.
21. Simon, S. L.; Mckenna, G. B.; Sindt, O. *J Appl Polym Sci* 2000, 76, 495.
22. Ratna, D.; Varley, R.; Simon, G. P. *J Appl Polym Sci* 2003, 89, 2339.
23. Adabbo, H. E.; Williams, R. J. *J Appl Polym Sci* 1982, 27, 1327.
24. Barone, L.; Carciotto, S.; Cicala, G.; Recca, A. *Polym Eng Sci* 2006, 46, 1576.
25. Cytec, Cycom 977-2 Toughened Epoxy Resin. <http://www.cytec.com/engineered-materials/products/Datasheets/CYCOM%20977-2.pdf> (accessed June 22, 2010).
26. Jumahat, A.; Soutis, C.; Jones, F. R.; Hodzic, A. *Compos Struct* 2010, 92, 295.
27. Hexcel, IM7 Carbon Fiber Product Data. http://www.hexcel.com/NR/rdonlyres/BD219725-D46D-4884-A3B3-AFC86020EFDA/0/HexTow_IM7_5000.pdf (June 22, 2010).